Electroencephalography and clinical Neurophysiology, 1983, 56: 38–51
Elsevier Scientific Publishers Ireland, Ltd.

DEMONSTRATION OF USEFUL DIFFERENCES BETWEEN MAGNETOENCEPHALOGRAM AND ELECTROENCEPHALOGRAM [1]

DAVID COHEN and B. NEIL CUFFIN

Francis Bitter National Magnet Laboratory, Massachusetts Institute of Technology, Cambridge, Mass. 02139 (U.S.A.)

(Accepted for publication: February 24, 1983)

The electrical sources in the brain not only produce an electric potential on the scalp, but also a magnetic field over the head (Cohen 1972). A recording of the potential is the well-known electroencephalogram (EEG), while a recording of the magnetic field is relatively new and is called the magnetoencephalogram (MEG). Although the MEG and EEG are produced by the same sources, an MEG map over the head shows a different spatial pattern than does an EEG map. These differences in the pattern may be useful, since they may allow the MEG to provide new information about the sources. Mostly for this reason, an increasing number of MEGs are being recorded (reviewed by Reite and Zimmerman 1978, and by Williamson and Kaufman 1981). Some of these recordings do suggest pattern differences which are useful; for example, they suggest that the MEG can better localize a source. However, these data are not conclusive. Theoretical studies have also been made which address these differences (Cuffin and Cohen 1979; Romani et al. 1982a). These studies, too, indicate useful differences. They predict pattern differences which, if true in actual recordings, would allow the MEG to better localize and differentiate the neural sources, in some ways, than does the EEG.

The purpose of this work is to perform a test and see if these predicted differences can be experimentally demonstrated. Demonstration is needed because the theoretical studies are based on spherical models of the head, and it is not known if the differences would be valid for the actual human head, with its various deviations from sphericity.

Because the type of source used theoretically for the predicted MEG-EEG differences is a current dipole, we seek to use the same source experimentally for our test. Ideally, the way to perform the test would be to implant an actual dipole in the human head and see if the same differences are seen in the experimental maps due to this dipole as in the theoretical maps. Obviously this is difficult to carry out. Instead, to perform our test, we here use a neural source which appears to behave as a dipole. This is the source of the N20 signal of the somatic evoked response, which occurs at about 20 msec following stimulation of the median nerve (Goff et al. 1977). This source is a good candidate for the test because its EEG map resembles that of a dipole (Allison 1982; Wood 1982), its approximate location is known (in the central sulcus), and it has been well studied both in scalp and cortical surface recordings (Allison et al. 1980; Broughton et al. 1981).

Our N20 maps are the first MEG and EEG maps recorded which can be compared conclusively, in that they are of the same subject, measured under the same conditions, and with adequate bandwidth. The form of EEG and MEG maps we basically use here is the monopolar form; by this we mean the common type of map, where at each point the EEG potential is measured with respect to a remote or inactive point, and the MEG is measured with a single coil. But because experimental monopolar maps can have significant errors, we also use the bipolar form of map as a backup; in this form, potential or magnetic field

[1] This work was supported by National Science Foundation Grant No. PCM-819973.

0013-4649/83/0000–0000/$03.00 Elsevier Scientific Publishers Ireland, Ltd.

differences between two adjacent points are mapped. Although not in common use, the bipolar maps offer verification of the monopolar results. However, the main idea of this paper can be understood if the reader chooses to omit the bipolar treatment.

In the following we first compare the theoretical monopolar MEG and EEG maps and show the differences which are predicted; then we do the same with the theoretical bipolar maps. We next show the N20 experimental monopolar maps and see if the same differences are seen, and finally do the same with the experimental bipolar maps.

Theoretical predictions (monopolar)

Most of the theoretical predictions were previously given in a form unsuitable for this experimental test [2]; therefore, we here recast those theoretical data into the map form we need. We use the same 4-sphere model used previously (Cuffin and Cohen 1979), which consists of a spherical 'brain,' over which there are 3 concentric spherical layers. The same method for computing the potentials and magnetic fields is used. The maps are shown in Fig. 1.

In the MEG map, the magnetic quantity most often measured is plotted; this is B_r, the radial component of the magnetic field vector $\vec{B}$. In the EEG map the potential V is plotted. The EEG maps are shown due to two tilt angles of the dipole: with and without a radial component. This is done in order to illustrate its effect. This component is important here because it theoretically cannot be seen on the MEG (Baule and McFee 1965); therefore the MEG map is due only to the tangential dipole component. In contrast, the radial component is readily seen on the EEG and plays a large role in MEG-EEG map differences.

[2] In Cuffin and Cohen (1979) the MEG and EEG spatial characteristics were given in the form where the measuring point on the head was fixed and the dipole location was varied to yield a lead field. What is needed here is the form where the dipole is fixed and the measuring point is varied to yield a map over the head.

We initially compare the MEG map in Fig. 1B to the EEG map due to the dipole without radial component in Fig. 1E. Each map is therefore due only to the tangential dipole. Although the patterns are roughly similar, we see two main differences. The first is that the pattern in the MEG map is rotated by 90° to that in the EEG map. This reflects a fundamental difference between the magnetic and electric field; their field vectors are generally perpendicular to each other. Although this 90° difference was obvious whenever B_r and V were plotted in previous studies, its significance was ignored. However, it is useful because it allows the MEG to more accurately locate a tangential dipole along a special direction than does the EEG; the advantage is reversed in the perpendicular direction. This is explained in Appendix A, where it is shown that each map has a preferred direction of localization, and the preferred direction in the MEG map is rotated by 90° to that in the EEG map. The MEG more accurately locates in the y direction, across the dipole, while the EEG does so in the x direction, along the dipole; in this way MEG and EEG are complementary.

The second difference is that the MEG pattern is somewhat tighter (more focal) than that of the EEG. The MEG peaks are seen to be 6 cm apart versus 9 cm for the EEG, hence the MEG pattern is one-third tighter. It has been shown (Cuffin and Cohen 1979) that the MEG pattern is tighter because the EEG measures the volume current which reaches the scalp, and this current has been smeared by the outer layers, especially by the high resistivity of the skull. In contrast, the MEG does not see the volume current (in addition to not seeing the radial dipole) hence 'does not know' about the outer layers; it sees only the tangential dipole itself (Cohen and Hosaka 1976). The MEG and EEG patterns would be about equally tight if the resistivity was uniform throughout the model. The use of the tighter pattern is to allow the MEG to more accurately locate a tangential source in its preferred direction than can the EEG in *its* preferred direction; this is understood using the concepts in Appendix A, where a tighter pattern results in a greater slope through the origin in Fig. 4.

We then compare the MEG map to the EEG map due to the dipole with radial component in

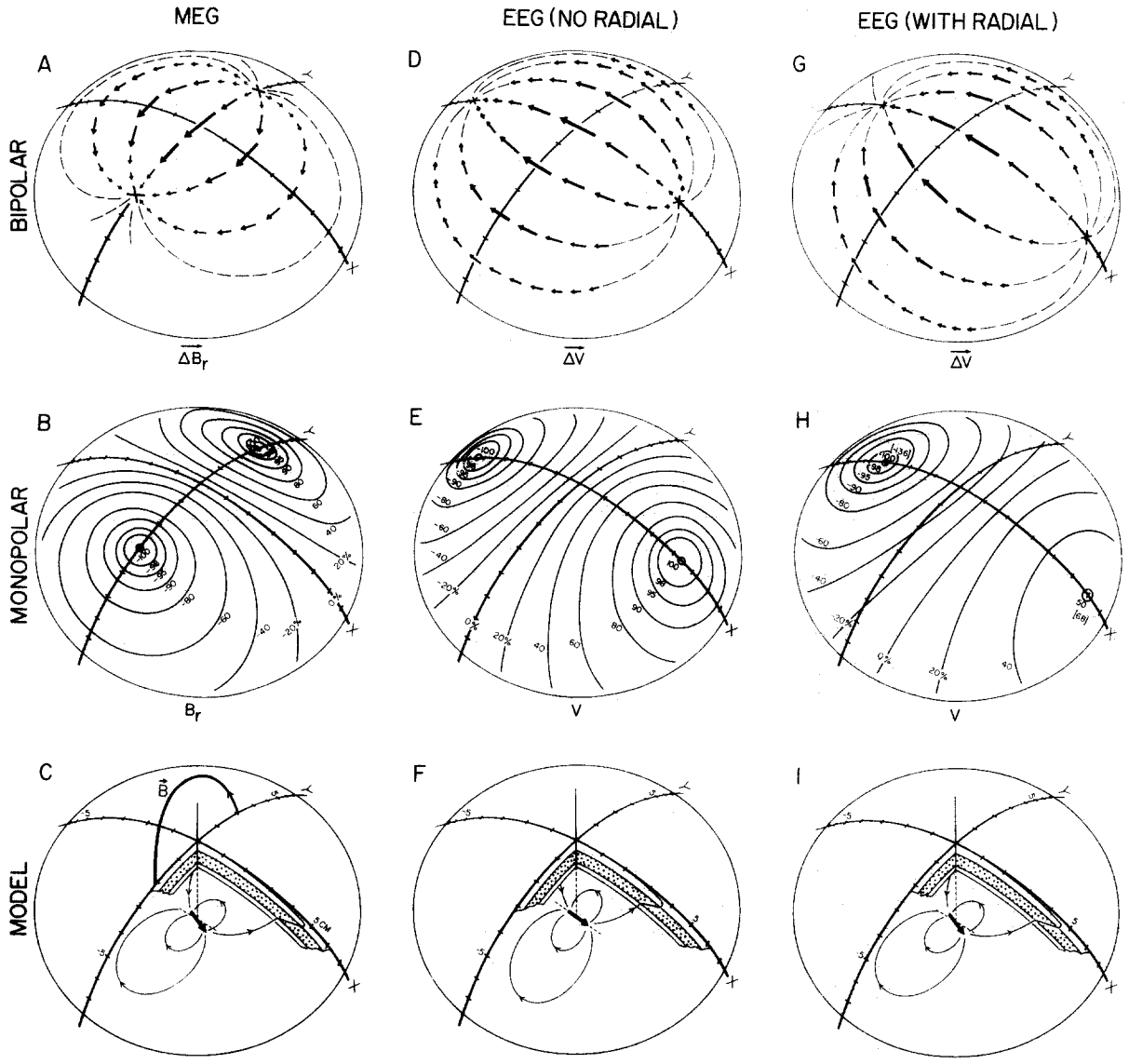

Fig. 1. Theoretical MEG and EEG maps due to a current dipole in a 4-sphere model of the head. In all panels only the upper cap of the sphere is shown, on which axes x and y (with 1 cm ticks) are fixed. The 3 model panels differ only in the orientation of the dipole (heavy arrow) which is tangential to x in F but tilted downward in C and I by 21°. The outer radius of the model is 9.5 cm; the layers are scalp, skull and cerebrospinal fluid, which have thicknesses of 0.32, 0.43 and 0.22 cm (resistivities in Appendix B); the inner sphere is the brain. The dipole depth is 2.7 cm. The magnetic quantity B_r (and $\Delta\vec{B}_r$) is computed using the actual sensing coil diameter, at 0.75 cm out from the sphere surface where the measurements are actually made. The reference point for V is on the sphere bottom. The monopolar peaks are located at ± 3.1 cm in B, ± 4.4 cm in E and $+6.1$ and -3.1 cm in H. In H, the percentages in parentheses are in terms of the peaks in E, showing that peak V is increased by 36% due to the dipole tilt. In the bipolar maps, the nulls (crosses) coincide with the monopolar peaks. The longest arrow in D is set equal to that in A, but in G it is scaled to that in D and is somewhat longer.

Fig. 1H. We see that the 90° rotation and tighter MEG pattern are maintained, but that there is now a third difference, in that the EEG pattern is now asymmetrical. Even though the downward angle of tilt of the dipole is only 21° from tangential, there has been a pattern shift of 1.5 cm in the +x direction and a change from a peak ratio of 1-to-1 to 2-to-1; this change includes an increase in peak value of 36% from that in Fig. 1E, which suggests the use of the third difference. We estimated that the peak increase would be 230% if this dipole were completely radial; further, because cortical sources are usually perpendicular to the cortical surface (Llinás and Nicholson 1974), those which are radial (to the skull) are in the gyri hence nearer to the scalp. It is therefore a reasonable assumption that the EEG map over the head is weighted by potentials due to radial sources, and that these potentials obscure those due to tangential sources. But the MEG does not see the radial dipole. This third difference, then, allows the MEG to reveal those tangential sources not discernible on the EEG when obscured by radial sources. Thus, when there are tangential sources in the vicinity of radial sources, the tangential sources would be clearly seen in the MEG, but would be obscured in the EEG by the radial sources.

Theoretical predictions (bipolar)

The theoretical bipolar maps are also shown in Fig. 1. Each bipolar measurement, called ΔB_r or ΔV, is the difference between two adjacent B_r or V measurements. These bipolar measurements are aligned in both the x or y directions. Each pair of crossed measurements, centered over a point, are combined as a vector located at that point on the map [3]. The bipolar map therefore shows the spatial rate of change or gradient of the corresponding monopolar map; thus a large vector at some point indicates that the monopolar quantity is changing rapidly in the direction of the vector at that point, while a vector of zero length indicates that the potential is constant about that point. Because it can be derived from the monopolar map, the bipolar map contains no new information. However, it emphasizes the sources nearest the skull because these produce the largest gradients, therefore it samples a group of sources distributed in depth differently than does the monopolar map. This is our main reason for using the bipolar map here; in the experimental N20 monopolar maps there may be significant error due to non-N20 sources at different depths, and the bipolar map can help discriminate against them.

We first compare the MEG map in Fig. 1A to the EEG map without radial in Fig. 1D. Although the peaks and nulls are reversed with those in the equivalent monopolar maps, the same two differences are present; the MEG pattern is rotated by 90° and is one-third tighter in comparison with the EEG pattern. We then look at Fig. 1G to see the effect of the radial component, and again note that the first two differences remain, and the EEG pattern has become asymmetrical. Hence the same 3 differences are present as in the monopolar maps. These differences have essentially the same use as in the monopolar maps, but because the peaks and nulls are reversed in the bipolar maps, there are minor variations. We consider, for example, the 90° difference. In localizing the dipole, the null points (monopolar peaks) are now the landmarks of importance instead of the monopolar null line; in the MEG map the source is located half-way between these points. However, the preferred directions remain as before. This is because the change in vector amplitude in passing through the nulls is different in x and y; in the MEG the rate of change is greater in y and in the EEG it is greater in x, hence the MEG localizes better in y via its nulls, while the EEG does so in x.

The reversal of the peaks and null points is here another reason we use the bipolar map. Because the position of a null generally can be more accurately found than that of a peak, the bipolar map can readily confirm the position of the monopolar peaks. These points are important here not only

[3] A MEG vector is defined as $\vec{\Delta B}_r = -(\Delta B_r/\Delta x)\vec{i} - (\Delta B_r/\Delta y)\vec{j}$ where Δx or Δy is the distance between adjacent measuring points and $\vec{i}$ and $\vec{j}$ are the x and y unit vectors. An EEG vector is similarly defined as $\Delta V = -(\Delta V/\Delta x)\vec{i} - (\Delta V/\Delta y)\vec{j}$. Previously (Cohen et al. 1980) we had combined the two magnetic bipolar values oppositely to that here, yielding the 'arrow,' which is at 90° to this MEG vector and has a special visual use.

for determining tightness of pattern, but also for localizing the source in the z direction (depth). This is done here by matching theoretical and experimental bipolar nulls (Appendix B); the monopolar peaks are used by others for this purpose as well (Romani et al. 1982a).

Experimental test (monopolar)

Two bald, male subjects were selected for this study; each was a paid volunteer and was measured, with his informed consent, during about 10 sessions. In each session the subject changed into apparel containing no magnetic material (zippers, nails in shoes, etc.), and a rectangular grid (1 cm × 1 cm) was marked on the left side of his head, centered at C_3 (International 10-20 system). About 30 EEG disc electrodes were then applied on the head in various arrays, usually 1.5 cm apart, and fed to 8 EEG amplifiers with filters. A stimulating electrode pair was pasted on the right wrist, and the current from a somatosensory stimulator (0.5 msec pulses) was adjusted to obtain a thumb twitch. All measurements were then made inside the MIT magnetically shielded room (Cohen 1972).

The MEGs were measured with the field-sensing coil shown in Fig. 2A, which was connected to a Superconducting Quantum Interference Device (SQUID). The coil and SQUID were located in a liquid helium dewar suspended from the ceiling, as previously described (Cohen 1972). For each measurement, the subject was comfortably seated with his head positioned very near the sensing coil in the dewar. The head was fitted into a cup of adjustable shape, fixed to the dewar. This set the position and angular orientation of the head, which was constantly checked during each measurement. The MEG noise was usually about 3 times greater than the corresponding EEG noise; while the MEG receives a smaller proportion of spontaneous brain signals because it sees a smaller volume and angular range of sources, the internal noise of our MEG system is perhaps an order of magnitude greater than that of the EEG. However, it is noteworthy that the MEG noise was less than that of the EEG when the recording site was directly over muscle, in the temporal region about T_3; although the EEG was heavily contaminated by the high-frequency myogenic noise, the MEG was almost free of this noise. (Because of this, the MEG could perhaps be used to determine if a latency component seen in the EEG is myogenic.)

The signals from the MEG and EEG channels were bandpass filtered to a frequency range of 0.3–300 Hz (rolloff about 12 dB/octave), where the MEG filters were carefully matched to those of the EEG. No other filtering, for example at 60 Hz, was necessary. The signals were fed into a computer for signal averaging; the sampling rate was 1300/sec. The signals were averaged over a period of 197 msec; the stimulation was applied 64 msec after the data-collection sweep began in order to obtain a meaningful prestimulus baseline. The stimulus was applied at the rate of about 1/sec, and either 100, 200 or 400 sweeps were averaged.

Experimental data are shown in Fig. 2. All the data shown here are from one subject; the data of the other subject were almost identical. In Fig. 2A the position of the axes on the head were defined by the positions of the peaks and nulls on the head. The positions for the raw traces were chosen to be at approximately equivalent points on the MEG and EEG preferred lines; the scales were chosen to equalize their amplitudes. These traces show that the N20 latency component (18.5 msec in this subject) is well defined, and that there are well-defined components at other latencies; these other components are different relative to the N20 component in the MEG than in the EEG. This is important because, unfortunately, there is spillover from the neighboring components into N20, which raises the question of whether or not the spillover is produced by sources at the same location as N20 and hence should be included in N20. The fact that these components are different in MEG and EEG indicates that their sources are of different location and/or orientation than N20, which suggests that they not be included in N20 and the spillover should be subtracted away. This method was supported by the fact that the maps produced using the subtractions were more dipole-like than those plotted without the subtraction. Because we wanted the most localized N20 source possible, we used this method for the data presented here.

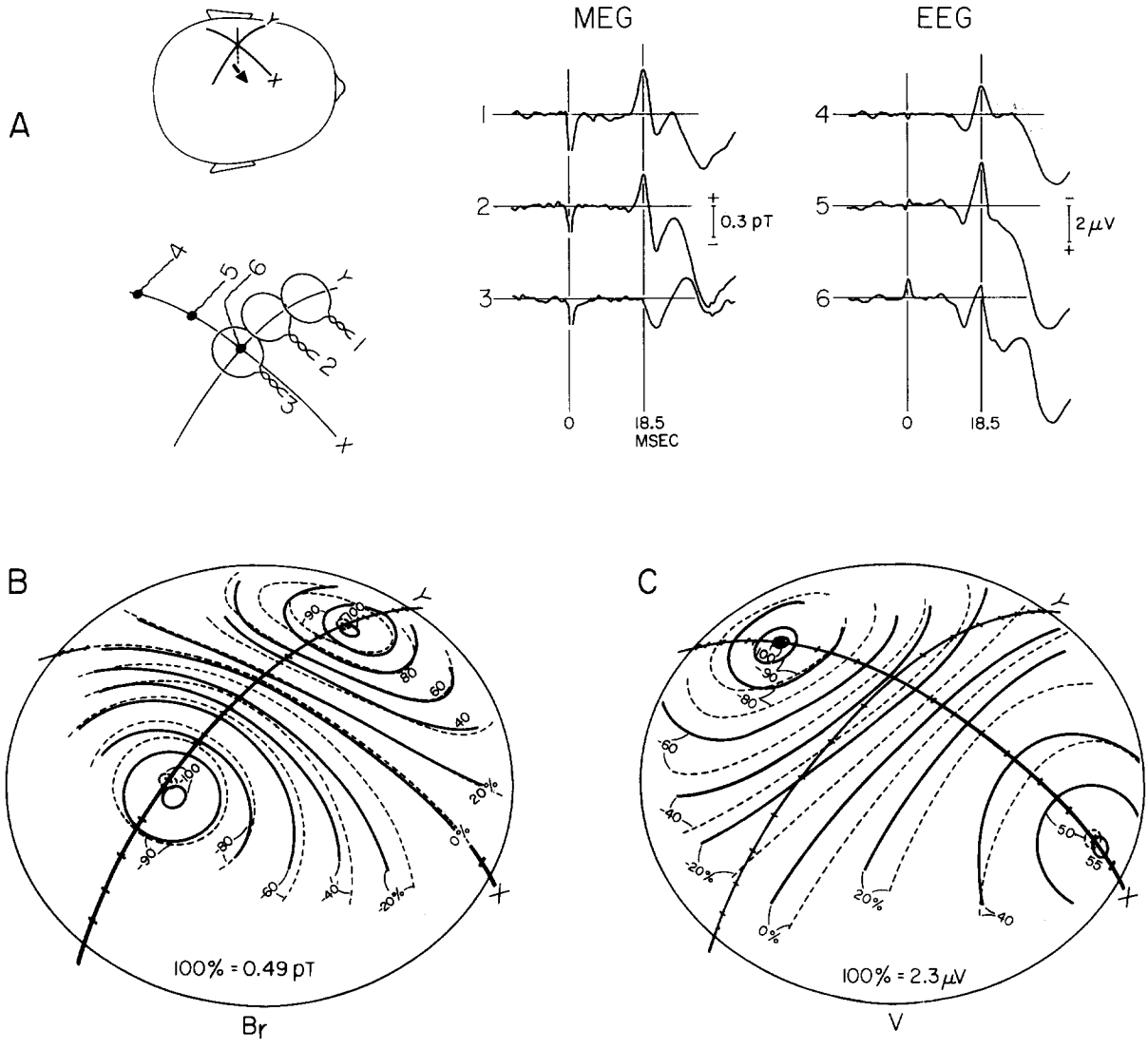

Fig. 2. Experimental (monopolar) data recorded from one subject. A: position of axes on his head, with expanded version below, and examples of raw traces recorded on these axes. The x-y origin is positioned 0.5 cm posterior-superior to C_3, and the x-axis is oriented at 52° to the lateral direction. The MEG coil which senses B_r, shown at 3 measuring locations 2.5 cm apart, is a circular loop 2.8 cm in diameter. The EEG electrode locations are 3.0 cm apart; the electrode is referenced to the joined ears. On the raw traces an artifact is seen where the stimulus is applied at zero time; the latency of the 'N20' signal for this subject is seen to be 18.5 msec. The number of sweeps averaged were 400 for the MEG and 200 for the EEG. The unit of B_r is the picotesla (pT), where 1 pT = 10^{-8} gauss. B and C: experimental maps of N20, shown as solid lines, superimposed on theoretical maps of Fig. 1B and H, shown as broken lines.

However, the subtraction of spillover became the major source of experimental error; this is because the percentage subtracted from N20 was occasionally large, especially in the EEG map, with correspondingly large uncertainty in the subtraction. In trace no. 6, for example, the spillover from both 15 and 22 msec into the 18.5 msec component is more than 50% of the N20 component, thereby yielding a large uncertainty in the final N20 amplitude.

The maps are shown in Fig. 2B and C. To produce these maps, the corrected 18.5 msec amplitude values were first plotted; points at about

48 MEG and 70 EEG locations over the head were used. Percentage contours were then drawn through the points. Because the various experimental errors show up as irregularities in these contours, they were smoothed in small degree to yield the contours shown here. We estimate the total experimental uncertainty in the percentage of each contour to be ±7% in MEG and ±10% in EEG, due mostly to spillover subtraction. By ±10% we mean that the amplitude range for, say, the 20% contour in Fig. 2C is 10–30%, where the probability for the true value to be outside these limits is very small.

Before comparing experimental MEG-EEG differences, we first verify that these experimental maps are indeed dipole-like; for this purpose, we will compare them generally to the theoretical maps on which they are superimposed. When the theoretical maps were computed, the dipole parameters and model resistivities were adjusted so that certain features of the theoretical maps matched those of the experimental maps; in this way the dipole best simulated our N20 source, and the experimental MEG-EEG differences could be most simply compared with the predicted differences. The details are described in Appendix B; briefly, the locations of the peaks in the theoretical maps were constrained to approximately coincide with those in the experimental maps. Otherwise the theoretical patterns are 'free,' and the experimental patterns can be compared to them. The experimental and theoretical patterns are seen to agree well in the MEG and adequately in the EEG map; the small mismatch in isomagnetic lines and the larger mismatch in isopotential lines are both within experimental error. The agreement in the ratio of EEG peak values (100-to-55 versus the theoretical 100-to-50) is convincing. Therefore we can say that the N20 source appears to behave as if it were a dipole in a spherical model, to within experimental error.

We can now proceed to see if the 3 MEG-EEG differences are demonstrated experimentally. First, we see that the MEG map is rotated by 90° to the EEG map. Second, we see that the MEG map has a tighter pattern than does the EEG map. Third, we see that the MEG map is symmetrical while the EEG map is asymmetrical. Thus, the theoretically predicted differences appear to exist experimentally. However, because of the error uncertainty, we remain doubtful, at least about the second difference. A small amplitude uncertainty produces a large error in position of the two peaks (Appendix A), hence in tightness of pattern; we estimate an uncertainty in peak position of ±1.0 cm in the MEG map and ±1.5 cm in the EEG map, hence it is conceivable that the MEG pattern is not significantly tighter. In order to verify the monopolar differences and remove any doubt, we consider the bipolar maps, where the error in position of the two equivalent points (nulls) is much less.

Experimental test (bipolar)

Although the bipolar maps can be mathematically derived from the monopolar maps, maps made this way would be very sensitive to noise, hence we instead recorded them separately. Thus, in a sense, they become independent measurements. The bipolar experimental arrangement was identical to the monopolar arrangement except for the configuration of coils and electrodes used at each measuring point. The MEG vector at each point is measured by two pairs of sensing coils, where one pair is perpendicular to the other; there are now 4 coils instead of one. Each pair is called a 2-D coil, and the system of both 2-D coils has been previously described (Cohen and Cuffin 1979; Cohen et al. 1980). One 2-D coil is shown in Fig. 3A. Both 2-D coils were coincident with the monopolar coil in the dewar tail. The two SQUID channels which they fed were processed identically and simultaneously with the monopolar channel. The EEG vector at each point is due to two crossed bipolar pairs; these two EEG channels were electrically treated in an identical way to the monopolar channels.

Some bipolar raw traces are shown in Fig. 3A. Recording locations were again chosen to be at approximately equivalent points on the MEG and EEG preferred lines, and scale factors chosen to produce equal amplitudes. Again the 18.5 msec component as well as those at other latencies are well defined, and again there is spillover into the 18.5 msec component. While the bipolar MEG

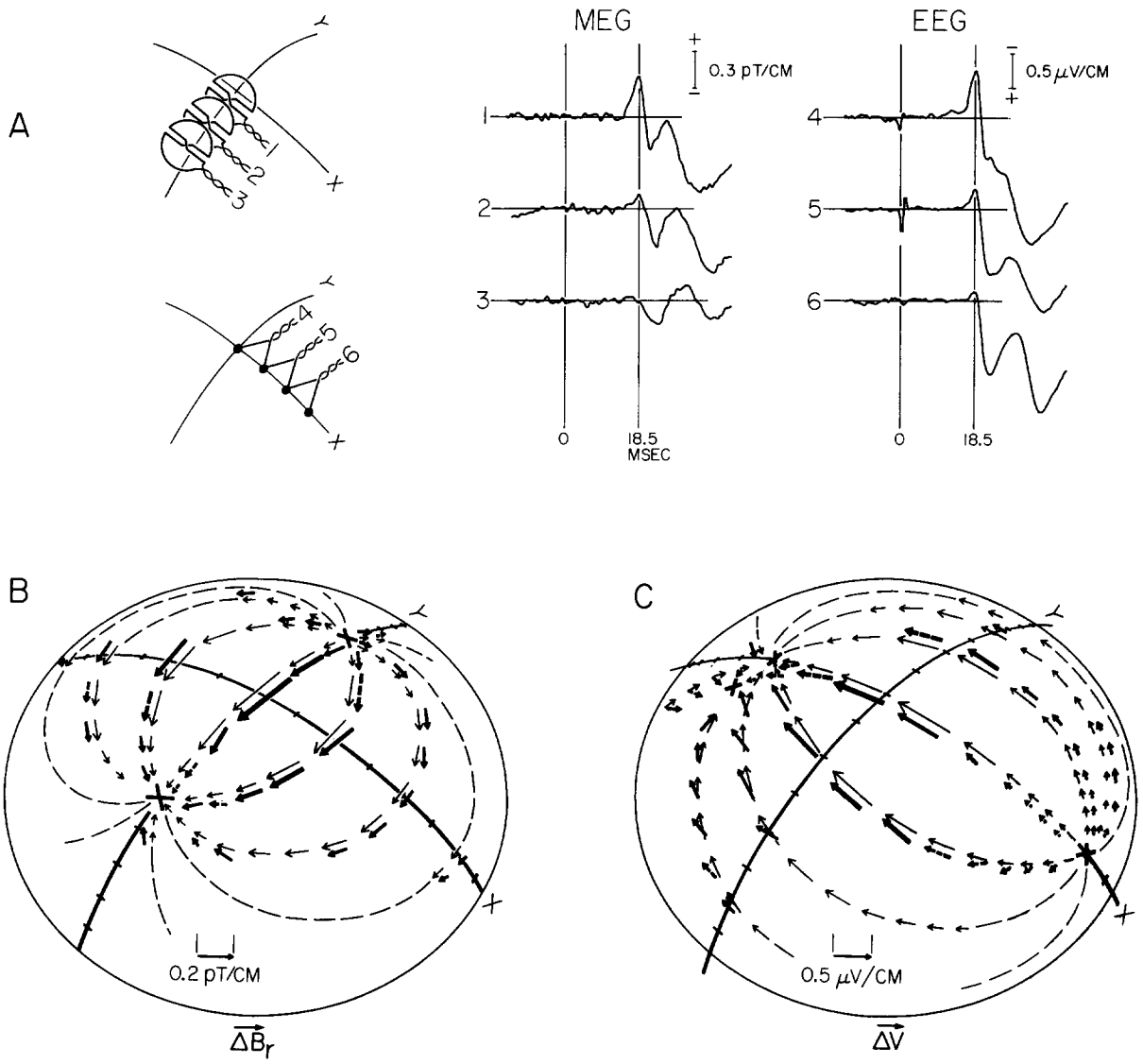

Fig. 3. Bipolar data of the same subject as in Fig. 2. A: examples of raw traces and recording locations. The MEG raw traces are due to one 2-D coil pair, 2.8 cm in diameter. The trace amplitude is proportional to ΔB_r, the difference in B_r between the D's. The effective distance between D's (Δy) is 1.5 cm. The EEG traces are due to one electrode pair, also 1.5 cm apart. Again 400 sweeps were averaged for MEG, and 200 for EEG. B and C: experimental maps of N20 (thick arrows) superimposed on theoretical maps of Fig. 1A and G, (thin arrows). Each MEG vector is measured with two superimposed 2-D coils, oriented at 90° to each other. The coil shown in A gives the x-component of the vector; the other coil, not shown, has D's aligned with y and gives the y-component. Each EEG vector is measured with two electrode pairs. The pair shown in A gives the x-component; the other pair, not shown, straddles this pair at 90° and gives the y-component. The scale vectors apply to both experimental and theoretical vector lengths. A broken experimental vector indicates that it was interpolated from data further away than 0.5 cm, hence may have some minor error. In B, the theoretical and experimental nulls (crosses) coincide, while in C they coincide at $+x$ but the experimental null is off-axis at $-x$.

non-N20 components are similar to those in the monopolar traces, in the EEG they are different; the monopolar component at about 15 msec is absent in the bipolar traces, while the large bipolar component at about 23 msec is smaller on the monopolar traces. Thus the bipolar EEG in these

traces views the sources differently than the monopolar EEG which, in part, justifies our use of the bipolar mode. The differences between the N20 and non-N20 components in these bipolar traces confirm the different locations and/or orientations of their sources and further support the method used in correcting spillover in the monopolar maps, which was also used here.

The experimental bipolar maps are shown in Fig. 3B and C. These maps were produced as before by first plotting the corrected amplitude values. Then interpolated arrows were plotted between these points, using minimal smoothing. As before, we first confirm that the experimental patterns are dipole-like by comparing them to the theoretical patterns on which they are superimposed. As noted in the monopolar case, some features of the theoretical maps had been matched to those in the experimental maps by adjusting the dipole parameters (Appendix B); these include the positions of the bipolar MEG nulls. However, the general theoretical patterns are again 'free,' and it is valid to compare the experimental patterns to them. It is again seen that they agree well in the MEG and adequately in the EEG; although the estimation of experimental uncertainty here is more complex than in the monopolar map, the agreement in general pattern is within experimental error when it is noted that the small mismatch in the EEG pattern is due only to the mismatch in the position of the far null. Therefore these maps are also dipole-like.

Next we compare experimental MEG-EEG differences. As in the theoretical bipolar maps there is 90° rotation, and the MEG pattern is about one-third tighter. We estimate an uncertainty in null position of about ± 0.4 cm in MEG and ± 0.6 cm in EEG, so that the MEG pattern is certainly tighter within experimental error. Finally, it is seen that the MEG pattern is symmetrical while the EEG pattern is asymmetrical. These independent measurements then confirm the differences seen in the monopolar maps.

Discussion

The 3 useful MEG-EEG differences, which are predicted for a dipole source, are seen to be experimentally demonstrated. But the predicted differences were here due to a theoretical dipole at a specific tilt angle and depth, and the demonstration was due to the specific neural source N20. We will therefore first comment on the generality or validity of this demonstration. Concerning the tilt angle and depth of the theoretical dipole, we state that the predictions in Fig. 1 do not depend on this choice of parameters. They are perfectly valid for all values of tilt angle and depth, except in two cases where the MEG does not see the dipole. The first, as we know, is where the dipole is oriented in a completely radial direction. The second, not yet mentioned, is where the dipole is located at the sphere center, in which case there is zero magnetic field around the sphere (Baule and McFee 1965).

Concerning our use of a specific neural source, we believe that the experimental differences seen here due to the N20 source should exist for other actual sources in the brain which are dipole-like. This is because we have here measured a dipole-like source at a 'bad location,' that is, at the side of a deep fissure. We would expect maps due to a source at this location to show the largest pattern distortions due to inhomogeneous regions in the brain; the inhomogeneity is here the conductivity change in passing tangentially across the fissure. Yet, to within experimental error, the same differences were seen as in the theoretical maps. Hence, the head appears to behave here as the spherical model. This is shown not only by the agreement in general pattern between experimental and theoretical maps, but also by the agreement between the values assigned for the theoretical dipole depth and model resistivities and the accepted values (Appendix B); had the head been unlike this model, we would expect unrealistic values in these parameters. It would appear, therefore, that the MEG-EEG pattern differences seen here with N20 should also apply to a dipole-like source at almost any location in the brain.

We next discuss the differences themselves. Both the first and second difference are useful for localization, therefore from this point of view we consider them together. In the first difference, it was noted that MEG and EEG each have a preferred direction of localization, and these are 90° apart; hence as far as localization is concerned, MEG

and EEG are complementary. To localize a dipole-like source in the x and y directions, both must be used. The MEG localizes best in y, while the EEG does so in x. In the second difference, it was determined that the MEG localizes better than the EEG, each in its own preferred direction; but it is only *somewhat better*. In the interpretation of MEG data from a dipole-like source, therefore, it cannot be claimed that the MEG truly localizes much better than does the EEG, no matter what the directions are of the measurements. Any dramatically better localization seen on the MEG could perhaps be due to measurements made along its preferred direction, in comparison to EEG measurements made along, say, its unpreferred direction, but this is not a valid comparison. MEG measurements should be made along its preferred direction and compared with EEG measurements along *its* preferred direction, and these would not show a large difference.

As an example, in Brenner et al. (1978), it is implied that the MEG shows much better localization than the EEG because it can resolve sources due to individual fingers over the somatosensory cortex. But we explain these results in the following way. If the source for each finger is effectively a dipole, and these are arranged side-by-side along the length of the central sulcus, then as different fingers are stimulated, the dipoles are switched along the MEG preferred line, hence readily resolved along this line; however, because the switch would be along the unpreferred direction of the EEG, the fingers would not be easily resolved by the EEG. Had the neuroanatomy been different, so that the finger dipoles were arranged in-line instead of side-by-side, then the EEG would have shown the better localization. Therefore the MEG localization is not truly much better; it is much better only in that particular situation.

We further consider the second MEG-EEG difference. Because the one-third tighter MEG pattern seen here pertains only to a particular coil diameter (2.8 cm) and only to the monopolar and bipolar coil configurations, it is important to know if a smaller coil diameter or a different coil configuration would yield a tighter pattern. Unfortunately, computations show (Cuffin and Cohen 1983) that as the coil diameter is decreased from 3.0 to 1.0 cm, the MEG pattern does not become significantly tighter for a dipole at this depth (2.7 cm) or greater. However, computations show that with quadrupolar coils (4 side-by-side loops) the pattern would be significantly tighter (Cuffin and Cohen 1979). Further, computations suggest (Cuffin and Cohen 1983) that a 'composite' 4-loop coil, consisting of a tilted (hinged) bipolar pair combined with a flat pair (such as the 2-D coil), can produce a significantly tighter pattern; there is therefore some possibility that tighter MEG patterns will be attained in the future by 4-loop coils.

With regard to the third difference, the symmetrical MEG map pattern in Figs. 2 and 3 indicates that it does not see the radial source component, at least to within experimental error (the explanation is given in Appendix C). Similar results were seen or suggested in two other cases. In the first, a 5 Hz theta wave was absent on a subject's MEG but was seen on the EEG, which showed a radial-like source pattern (Cohen 1972). In the second, the fact that the MEG does not see the radial dipole component was used in the explanation of the polarization of the MEG alpha rhythm (Cohen and Cuffin 1979). That it does not see this component also calls attention to an interesting consequence, suggested previously in that paper. If the MEG does not see this component, then it should only be able to see sources which are located in the sulci of the cortex, not the gyri; the sources in the gyri should be invisible to the MEG. This is because the sources, usually perpendicular to the cortical surface (Llinás and Nicholson 1974), should be tangential to the skull only in the sulci, hence visible to the MEG, but radial to the skull in the gyri, hence invisible to the MEG.

That it does not see this component relates indirectly to the above discussion on localization. One effect can be that the area on the scalp over which a latency component can be measured by the MEG is shrunk in comparison to the EEG, giving the illusion of dramatically better MEG localization. For example, presently we are studying the MEG versus the EEG map of N100 of the auditory evoked response and have noticed that the MEG pattern for one subject is mugh tighter than is the EEG pattern. Although it appears that the MEG is localizing N100 much better than is

the EEG, in fact the explanation could well be that there are radial N100 sources distributed over a wide area of cortex, but only a few tangential sources in a small region. Stated otherwise, MEG and EEG are not seeing the same sources; the MEG here sees only the confined, tangential sources, while the EEG also sees the radial sources over the wide area.

Concerning the use of the third difference, that the MEG can reveal tangential sources obscured in the EEG, it cannot be applied to presently published MEG results. This is because in the cases where new MEG phenomena are claimed to be seen, which perhaps could be explained as tangential dipoles obscured in the EEG, there are no adequate EEG data for comparison; for example, in the MEG visual phenomena in Williamson et al. (1978), or in the MEG auditory phenomena in Romani et al. (1982b). We can only speculate that this third MEG-EEG difference will explain some of this when further data are accumulated.

Finally, we comment on MEG-EEG differences for sources which are not dipole-like; most electrical sources in the brain are in this non-dipolar class. For these sources, the 3 differences seen here may not exist. Each of these sources can be approximated by two or more dipoles, therefore there are many cases to consider because there are many possible dipole combinations. Some special cases have already been studied theoretically; in these the sources consisted of two dipoles either exactly in-line or side-by-side (Cohen and Hosaka 1976). Some dramatic map differences were seen in these two cases, but there may not be many actual neural sources which can be approximated in this way. Further, the model used in that study was only a semi-infinite volume conductor. The study of such cases should therefore be enlarged and refined using the 4-sphere model; because of the experimental-theoretical agreement seen here, this model can now be used quite confidently to compute MEG and EEG maps. Thus, the experimental demonstration presented here not only confirms the useful differences for a dipole-like source, but also provides the basis for the analysis of more complicated cases.

Summary

For a dipole source, theory predicts 3 useful differences between the MEG and EEG spatial patterns over the head. These are seen when a comparison is made between theoretical MEG and EEG maps, due to the dipole in a spherical model of the head. If true, these differences would allow the MEG to better localize or differentiate neural sources in some ways than does the EEG. A first experimental test of the differences is made here. A comparison is made between MEG and EEG maps due to a neural source which appears to behave as a dipole (N20 of the somatic evoked response). The same 3 differences are seen, therefore the predicted differences are confirmed experimentally. The first 2 differences, due only to the tangential component of the dipole, are that the MEG pattern is rotated by 90° from the EEG pattern and is one-third tighter. The first allows the MEG to localize a tangential dipole better in a preferred direction, across the dipole (while the EEG does so along the dipole); the second allows the MEG to localize somewhat better in its preferred direction than the EEG does in its preferred direction. The third difference is due only to the radial component of the dipole; while the MEG receives no contribution from this component, the EEG pattern is asymmetrical and is heavily weighted by it. This allows the MEG to reveal tangential sources which are obscured by the radial sources in the EEG. For sources which cannot be approximated by a dipole, the MEG-EEG differences will depend on the particular case; however, the spherical model can now be used with more confidence to predict differences in these cases.

Résumé

Démonstration de différences utiles entre magnétoencéphalogramme et electroencéphalogramme

Pour une source en dipôle, la théorie prévoit 3 différences utiles entre les patterns spatiaux MEG et EEG sur le crâne. Elles apparaissent lorsqu'une comparaison est effectuée entre cartes théoriques

MEG et EEG, produites par un dipôle dans un modèle sphérique de la tête. Si ces différences sont réelles, le MEG pourrait d'une certaine façon mieux localiser ou distinguer les sources nerveuses que l'EEG. Une première épreuve expérimentale de ces différences est présentée ici. Une comparaison est effectuée entre les cartes MEG et EEG pour une source nerveuse qui semble se comporter comme un dipôle (l'onde N20 de la réponse évoquée somatique). Les 3 mêmes différences ont été observées, ce qui est une confirmation expérimentale. Les 2 premières différences, uniquement dues à la composante tangentielle du dipôle montrent que le pattern du MEG subit une rotation de 90° par rapport au pattern EEG ainsi qu'un resserrement d'un tiers. La première différence permet au MEG de mieux localiser un dipôle tangentiel dans une direction 'préférentielle' à travers le dipôle (tandis que l'EEG le fait le long du dipôle); la seconde permet au MEG une meilleure localisation dans sa direction préférentielle que l'EEG dans la sienne. La troisième différence est due uniquement à la composante radiale du dipôle; tandis que le pattern EEG est insensible à cette composante, le pattern EEG est assymétrique et massivement influencé par cette composante. Cette propriété permet au MEG de mettre en évidence des sources tangentielles masquées par des sources radiales dans l'EEG. En ce qui concerne les sources ne pouvant pas être assimilées à un dipôle, les différences MEG-EEG varient pour chaque cas; mais pour chacun d'eux, le modèle sphérique peut maintenant être utilisé avec plus de confiance pour prédire les différences.

Appendix A

The purpose here is to show that there is a preferred direction for localization of a tangential dipole in both MEG and EEG monopolar maps; also, to show that the preferred direction in the MEG map is oriented at 90° to that in the EEG map. We proceed by asking this basic question: How well can we locate the x and y positions of the dipole by using either the MEG or the EEG maps? The answer depends on the experimental uncertainty in each map. In the ideal case of no uncertainty in B_r or V, there would be no uncertainty in the x and y dipole positions; they could be determined with complete accuracy from, say, the x and y positions of the peaks. In the realistic case there is experimental uncertainty, and hence uncertainty in determining the dipole's position. Fig. 4 illustrates how amplitude uncertainty in a map translates to position uncertainty. The amplitude uncertainty, which is assumed to be a constant ±10% of the peak, defines a band about the two solid curves. But this band also indicates, at any particular amplitude, an uncertainty in the x or y position; this is identical to uncertainty in the dipole location if we imagine the map to be fixed to the dipole. This uncertainty, shown as a horizontal bar, is not constant but depends on the part of the curve used. The least uncertainty (shortest horizontal bar) is where a curve has the most rapid rate of change, which is seen to occur at the zero-crossing; hence the direction or cut-line on the map which allows this zero-crossing is called preferred. This is y for the MEG and x for the EEG, therefore the MEG preferred direction is at 90° to that of the EEG. If, instead, one attempted

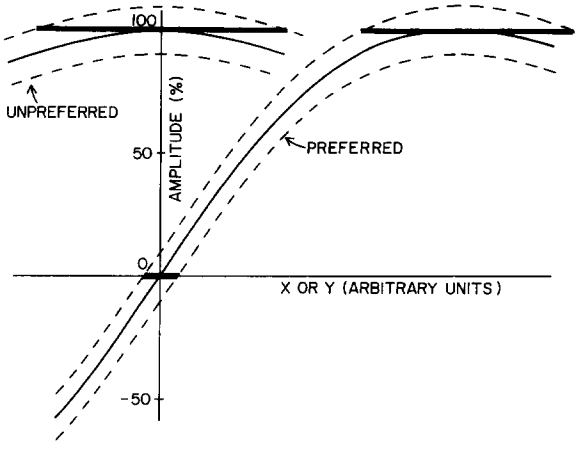

Fig. 4. Solid curves are B_r or V versus x or y in the theoretical monopolar maps. The preferred solid curve is due to a cut either along the y-axis in Fig. 1B or along the x-axis in Fig. 1E. The unpreferred is due to a cut through the + peak, at 90° to the preferred cut, hence it is parallel to (but displaced from) the x-axis in Fig. 1B and to the y-axis in Fig. 1E. The broken lines define a band of amplitude uncertainty which is ±10% of maximum; the 3 horizontal bars show the resulting x or y uncertainty at the origin and at a peak.

to localize along this line by using its peaks, the bar length is seen to be much greater. If one localized in the 90° direction, there is no choice but to use the peaks; on the line used, parallel to but displaced from an axis, the bar length is greater yet, hence this direction is called unpreferred.

Appendix B

We describe how the model parameters were adjusted so that the theoretical monopolar and bipolar maps were a reasonably good match to the experimental N20 maps. First the dipole depth was assigned. This was done by exactly matching the two null positions in the bipolar MEG theoretical map to those in the experimental map; as noted, these null positions correspond to the two peak positions in the monopolar maps, but are more accurately determined in the bipolar map (see Appendix A). The value assigned was 2.7 cm, which is in agreement with its location in the central sulcus (Allison 1982). Then the tilt angle of the dipole, hence its radial component, was assigned (21°). This was done by approximately matching the null positions of the theoretical EEG bipolar map to those of the experimental map; due to the radial dipole, these are situated asymmetrically. Next, the dipole strength was assigned (2.1 μA-cm). This was done by choosing a strength which produced agreement between the maximum B_r value in the theoretical and experimental MEG monopolar maps; using this value, the value of the largest vector in the theoretical bipolar MEG map was found to agree with its experimental counterpart to within 10%, which was within experimental error. Finally, the resistivities in the model were assigned. This was done by adjusting them so that the maximum potential in the theoretical monopolar EEG map matched its experimental counterpart; using these values, the value of the largest vector in the theoretical bipolar EEG map agreed with its experimental counterpart to within several per cent, which was certainly within experimental error. For the resistivities of scalp, skull, fluid and brain, the following values were assigned (in Ω-cm): 217, 17,200, 72, and 217; these are in the range of accepted values (Geddes and Baker 1967).

Appendix C

We argue that the symmetrical MEG pattern seen in Fig. 2 (and Fig. 3) indicates that the MEG does not see the radial component of the source. We first consider a radial dipole in our model of 4 concentric spheres; it produces $\vec{B} = 0$ externally. Next we place a rectangular plate alongside the dipole and parallel to it in the inner sphere, but of different conductivity; as a result, the circular symmetry of the volume current about the dipole is destroyed. The current will now be asymmetrical about an imaginary plane through the dipole and parallel to the plate. Thus, an external B_r has been created which is asymmetrical about this plane. Therefore if there was a purely radial dipole in a head which consisted of purely spherical layers plus a fissure near the dipole (the plate), then an MEG pattern would be created which would be asymmetrical about the plane parallel to the fissure. More generally, if there was a tilted dipole in the head, as is effectively the case with N20, then a fissure (plate) would both create this MEG asymmetrical pattern due to the radial component, and alter the MEG pattern due to the tangential component so that it was also asymmetrical about the same plane; the radial asymmetrical pattern would be superimposed on that of the tangential component. Now in the case of our N20, the central sulcus (Rolandic fissure) is parallel to the y axis, hence our imaginary plane coincides with the y axis, and if there was any MEG asymmetry due to the fissure we would see it about this axis. However, the MEG pattern in Fig. 2 (and Fig. 3) is seen to be symmetrical about y to within experimental error; that is, the effect of the fissure is less than the experimental error. Hence, to within the accuracy of our MEG mapping, the head appears to behave as a spherical model and the MEG does not see the radial source component.

We thank T. Allison and C.C. Wood for their advice. We also thank T. Teyler for his encouragement during the early phases of the project.

References

Allison, T. Scalp and cortical recordings of initial somatosensory cortex activity to median nerve stimulation in man. Ann. N.Y. Acad. Sci., 1982, 388: 671–678.

Allison, T., Goff, W.R., Williamson, P.D. and Vangilder, J.C. On the neural origin of early components of the human somatosensory evoked potential. In: J.E. Desmedt (Ed.), Progress in Clin. Neurophysiol., Vol. 7. Karger, Basel, 1980: 51–68.

Baule, G. and McFee, R. Theory of magnetic detection of the heart's electrical activity. J. appl. Physiol., 1965, 36: 2066–2073.

Brenner, D., Lipton, J., Kaufman, L. and Williamson, S.J. Somatically evoked magnetic fields of the human brain. Science, 1978, 199: 81–83.

Broughton, R., Rasmussen, T. and Branch, C. Scalp and direct cortical recordings of somatosensory evoked potentials in man (circa 1967). Canad. J. Psychiat., 1981, 35: 136–158.

Cohen, D. Magnetoencephalography: detection of the brain's electrical activity with a superconductivity magnetometer. Science, 1972, 175: 664–666.

Cohen, D. and Cuffin, B.N. Magnetic measurement and display of current generators in the brain. Part II. Polarization of the alpha rhythm. Proc. XII Int. Conf. Med. Biol. Engng, 1979: 17–18.

Cohen, D. and Hosaka, H. Magnetic field produced by a current dipole. J. Electrocardiol., 1976, 9: 409–417.

Cohen, D., Palti, Y., Cuffin, B.N. and Schmid, S.J. Magnetic fields produced by steady currents in the body. Proc. natl. Acad. Sci. (Wash.), 1980, 77: 1447–1451.

Cuffin, B.N. and Cohen, D. Comparison of the magnetoencephalogram and electroencephalogram. Electroenceph. clin. Neurophysiol., 1979, 47: 131–146.

Cuffin, B.N. and Cohen, D. Effects of coil size on MEG measurements. J. appl. Phys., 1983, 54: in press.

Geddes, L.A. and Baker, L.E. The specific resistance of biological material — a compendium of data for the biomedical engineer and physiologist. Med. biol. Engng, 1967, 5: 271–293.

Goff, G.D., Matsumiya, Y., Allison, T. and Goff, W.R. The scalp topography of human somatosensory and auditory evoked potentials. Electroenceph. clin. Neurophysiol., 1977, 42: 57–76.

Llinás, R. and Nicholson, C. Analysis of field potentials in the central nervous system. In: A. Rémond (Ed.), Handbook of Electroencephalography and clinical Neurophysiology, Vol. 2B. Elsevier, Amsterdam, 1974, 61–83.

Reite, M. and Zimmerman, J. Magnetic phenomena of the central nervous system. Ann. Rev. biophys. Bioengng, 1978, 7: 167–188.

Romani, G.L., Williamson, S.J. and Kaufman, L. Biomagnetic instrumentation. Rev. Sci. Instrum., 1982a, 53: 1815–1845.

Romani, G.L., Williamson, S.J. and Kaufman, L. Tonotopic organization of the human auditory cortex. Science, 1982b, 216: 1339–1340.

Williamson, S.J. and Kaufman, L. Biomagnetism. J. Magn. Magn. Mat., 1981, 22: 129–202.

Williamson, S.J., Kaufman, L. and Brenner, D. Variation with spatial frequency in the latency of the neuromagnetic response of the human visual cortex. Vision Res., 1978, 18: 107–110.

Wood, C.C. Application of dipole localization methods to source identification of human evolved potentials. Ann. N.Y. Acad. Sci., 1982, 388: 139–155.